Food Research International 223 (2026) 117840

Contents lists available at ScienceDirect

Food Research International

journal homepage: www.elsevier.com/locate/foodres

In vitro antitumor activity of *Lactococcus lactis* cell-free supernatant on human glioblastoma cell lines

I. De Chiara [a], A. Feola [b], M. Della Gala [a], R. Marasco [a], M.S. Nielsen [c], A. Porcellini [b], M. Grieco [a], M.T. Gentile [a,*], L. Muscariello [a,*]

[a] Department of Environmental, Biological and Pharmaceutical Sciences and Technologies (DiSTABiF), University of Campania Luigi Vanvitelli, Caserta, Italy
[b] Department of Biology, University of Naples "Federico II", Laboratory of General and Clinical Pathology, Naples, Italy
[c] Department of Biomedicine, Faculty of Health, Aarhus University, 8000 Aarhus C, Denmark

ARTICLE INFO

Keywords:
Probiotics
Postbiotics
Lactococcus lactis
Glioblastoma
cancer therapy
Blood-brain barrier

ABSTRACT

In the last few years, probiotics have gained much attention within the medical, pharmaceutical, and food fields, given the health benefits provided by their consumption. They include several lactic acid bacteria (LAB) species, mostly belonging to the genera *Lactobacillus*, *Lactococcus*, and *Streptococcus*. Postbiotics are bioactive compounds (organic acids, short-chain fatty acids, enzymes, and neurotransmitters) produced by bacterial fermentation that exert different health effects. It is well known that probiotics, as health-promoting microorganisms, show different therapeutic properties, including anti-pathogenic, anti-inflammatory, and cholesterol-lowering activities. Recently, accumulating evidence has shown that certain commensal bacteria play protective roles against cancer; thus, anti-carcinogenic activity is one of the most interesting probiotics properties that is currently under investigation. Here, we studied the *in vitro* anticancer properties of postbiotics produced by three different *Lactococcus lactis* subsp. *lactis* strains isolated from natural whey starter cultures on human glioblastoma cell lines. MTT and trypan blue exclusion assays revealed a significant reduction in cell proliferation, and flow cytometry analysis corroborated this data, demonstrating a cell cycle arrest in treated cells. Moreover, other cancer hallmarks, such as wound healing rate closure and migration, were markedly inhibited by postbiotics. On the other hand, primary astrocytes viability and the blood-brain barrier (BBB) integrity were not impaired, suggesting a selective effect of postbiotics on proliferating-undifferentiated cells. This preliminary *in vitro* study highlights, for the first time, the potential anticancer properties of postbiotics from some *L. lactis* strains on human glioblastoma cell lines

1. Introduction

Lactic acid bacteria (LAB) are generally recognized as safe, active, and functional ingredients for food production and preservation. LAB-derived fermented food has been an important component of the human diet for millennia (Vera-Santander, Hernández-Figueroa, Jiménez-Munguía, Mani-López, & López-Malo, 2023). They are important constituents of human microbiota and include many probiotic strains. Well-documented health-promoting effects of LAB include the improvement of gastrointestinal disorders and bacterial vaginosis, as well as treatment of allergies, obesity, and depression (Leo et al., 2023; Sebastián Domingo, 2017; Wu et al., 2023). Recently, several evidence suggested that gut microbial balance may contribute to cancer prevention and help the effectiveness of anti-cancer therapies. Modulation of gastrointestinal microflora, enhancement of the host's immune response, induction of apoptosis, antioxidative, and antiproliferative properties are among the mechanisms of action linked to probiotics to exert their anticancer effect (Abd Ellatif et al., 2022; Chuah et al., 2019; Sharma, Kaur, Kaur, & Kaur, 2018). Recently, health-promoting LAB strains have also been proposed for the production of postbiotics, namely, water-soluble products deriving from bacterial metabolism or being by-products from bacterial cells after their lysis. Postbiotics, produced by microbiota-beneficial bacteria, represent last-generation health-promoting molecules showing different advantages since they are more stable and safer than probiotics. Indeed, they should not be subjected to the same safety measures as products that include live microorganisms (Nataraj, Ali, Behare, & Yadav, 2020; Scott, De Paepe, & Van de Wiele, 2022). In addition to cell-free supernatants (CFSs) from

* Corresponding authors.
E-mail addresses: mariateresa.gentile@unicampania.it (M.T. Gentile), lidia.muscariello@unicampania.it (L. Muscariello).

https://doi.org/10.1016/j.foodres.2025.117840
Received 18 June 2025; Received in revised form 29 October 2025; Accepted 10 November 2025
Available online 25 November 2025

bacterial fermentation, postbiotic components include also microbial molecules and metabolites such as short-chain fatty acids (SCFAs), enzymes, peptides, teichoic acids, peptidoglycan-derived muropeptides, *endo*- and exopolysaccharides (EPSP), cell surface proteins, vitamins, plasmalogens, and organic acids. For this reason, CFSs could be proposed as adjuvant in oncology (Banna et al., 2017). Several preclinical studies demonstrated their capability to effectively arrest cancer cell growth, both *in vitro* and *in vivo* in several cancer types including oral, colon, cervical, and breast cancer. CFSs and EPSP from *Lactobacillus* and *Bifidobacterium* species were found to inhibit colon cancer progression and induce apoptotic cell death (Song, Wang, Ma, Liu, & Wang, 2023). Previously, Liu and co-workers (2012) showed that EPSP from LAB had anti-oxidative properties and antiproliferative effects on hepatoma HepG2 cells (Eladwy et al., 2024; Elango, Nesam, Sukumar, Lawrence, & Radhakrishnan, 2024; Liu et al., 2012; Scott et al., 2022). Several studies demonstrated the therapeutic potential of SCFAs in protection against colorectal, pancreatic and gastric cancer (Eladwy et al., 2024; Elango et al., 2024; Song et al., 2023). Postbiotics from *Lactobacillus plantarum* strains showed an inhibitory effect on the proliferation of human breast cancer cells (Chuah et al., 2019). Although preclinical studies suggest that oral administration of postbiotics exhibits beneficial effects against various types of cancer, nowadays, nothing is known about the effect of postbiotics on brain cancers yet (Eladwy et al., 2024; Elango et al., 2024; Song et al., 2023). Among brain tumors, glioblastoma multiforme (GBM) represents the most common and most aggressive subtype of glioma, with an overall incidence of less than 10 per 100,000 people, representing approximately 15 % of brain tumors. In recent years, the number of GBM cases in adulthood or young adulthood is continuously rising. Due to the early invasion of the brain parenchyma, its complete surgical removal is almost impossible. Currently, therapeutic approaches consist of surgical resection followed by radiotherapy and chemotherapy. Drugs used to treat GBM are temozolomide (TMZ) and cisplatin (Zou et al., 2022), the first-choice cytotoxic agents for gliomas, that alkylate the DNA of both cancer and normal cells. However, tumors treated with TMZ soon develop chemo-resistance largely due to several mechanisms such as the activation of alternative DNA repair systems, epigenetic modifications (high methyl-guanine methyltransferase (MGMT) levels), the inactivation of mismatch repair enzymes MLH1 and MSH29, and over-expression of multidrug resistance proteins (Singh, Miner, Hennis, & Mittal, 2021). Moreover, one of the worst side effects of TMZ chemotherapy is represented by cognitive impairment such as loss of memory and learning, which is even more severe in the case of childhood brain (Zou et al., 2022). Although the underlying cellular and molecular mechanisms are largely unknown, these effects, often referred to as “chemo-brain”, are due to the alkylating property of these drugs which target the DNA of both cancer and healthy cells. Therefore, identifying new more effective, and non-toxic compounds represents an urgent need in the therapy of GBM. The investigation of the gut microbiome’s relationship with the brain is a rapidly evolving field, which may lead to potential therapeutic avenues for a disease with limited treatment efficacy. Here, we reported the biological effects of CFSs from three different *Lactococcus lactis* subsp. *lactis* strains, previously isolated from natural whey starter culture (De Chiara et al., 2024), on different glioblastoma cell lines. In particular, we tested the ability of CFSs to inhibit proliferation, cell cycle, migration, and tumorosphere formation in GBM cell lines. We also show that the tested CFSs are non-toxic on healthy primary astrocytes and on an *in vitro* model of BBB, preserving its integrity.

2. Results

2.1. Lactococcus lactis cell-free supernatants (CFSs) impair cell viability of glioblastoma cell lines

CFSs derived from eight different L. *lactis* strains (A3, A5, B1, D1, D3, I1, I4, I7) were used to preliminarily test, by MTT assay, their effect on U87MG cell proliferation. A dose-dependent (50, 5, 0.5 mg/mL) and time-course analysis (24, 48, 72 h) was performed (Supplementary Fig. S1). Based on previous results concerning probiotic properties (De Chiara et al., 2024) and the effect of CFSs on U87MG cell proliferation, D1, I4, and I7 *L. lactis* strains were selected for further analysis, performed also on U251 and T98 cell lines, at the lowest concentration tested (0.5 mg/mL). As shown in Fig. 1a, no differences were detected 24 h after treatment when compared to untreated cells for any of the three CFSs on U87MG. A decrease in cell viability was observed 48 h (42, 50, and 55 % for D1, I4, and I7, respectively), and 72 (53, 83, and 45 %) hours after CFSs administration as compared to the untreated cells (Fig. 1a). Similar effects were also observed on the U251 cell line (Fig. 1b). On the contrary, CFSs of D1, I4, and I7 strains did not affect T98 cells, in which an increase in cell viability was observed (Fig. 1c). This resistance in T98 cells is likely due to the upregulation of efflux transporters and enhanced DNA repair mechanisms, which could mitigate the cytostatic effects of the CFSs (Nakatsuma et al., 2010). MTT data were further supported by the Trypan blue exclusion assay. Cells were stained, counted, and reported as number of live/dead cells. Untreated cells were used as a positive control. CFS of L. *lactis* D1, I4, and I7 decreased the cell viability of U87MG cells at a concentration of 0.5 mg/mL after 24 h (Fig. 1d). Contrariwise, no significant effects between live and dead cells were observed in the other two cell lines (Fig. 1e, f). Taken together, these data indicate a cytostatic effect of the three selected CFSs, rather than cytotoxic.

2.2. CFSs from L. lactis D1-I4-I7 arrest proliferation in various cell cycle phases, but do not induce apoptosis

To test the effects of the CFSs from D1, I4, and I7 strains on the cell cycle progression, U251, U87MG, and T98 cell lines were treated or not with CFSs for 12 and/or 24 h. Results demonstrate that all the treatments induce an arrest of glioblastoma cell cycle in different phases. Particularly, D1, I4, and I7 treatments on U251 induce a weak decrease of G0/G1 phase in 12 h compared to the control. On the other hand, more than 5.0 % (27.8 % ± 1.0 *Vs* 22.6 % ± 0.8), 7.0 % (29.0 % ± 0.5 *Vs* 22.6 ± 0.8) and 8.0 % (30.0 % ± 0.5 *Vs* 22.6 % ± 0.8) of cells, respectively, begin to accumulate in G2/M phase compared to the untreated control (Fig. 2). However, 24 h after D1 and I4 treatments, U251 cells are arrested in G2/M, while 24 h after I7 treatment (Fig. 2a and Supplementary fig. S2), the cells re-enter the S-phase, starting a new cell cycle. In U87MG cells, treatment with D1 and I7 CSFs for 12 h, induce an accumulation in G0/G1 phase of about 12.0 % (45.8 % ± 0.4 *Vs* 34.2 ± 1.0) and 7.5 % (41.7 % ± 0.3 *Vs* 34.2 ± 1.0), respectively; and in G2/M phase of about 8.4 % (32.9 % ± 1,0 *Vs* 24.5 % ± 0.8) and 5.9 % (30.4 % ± 0.5 *Vs* 24.5 % ± 0.8), respectively. Consequently, a decrease of about 10 % in the S-phase is observed. I4 treatment does not show statistically significant differences in the cell cycle phases compared to control conditions (Fig. 2b). Concerning T98 cells, D1 and I4 CFSs show an increase of about 12 % in G0/G1 phase (67.0 % ± 0.5 *Vs* 55.6 ± 0.8) and 11.0 % (66.5 % ± 0.5 *Vs* 55.6 % ± 0.8), respectively, compared to control (Fig. 2b,c). In contrast, I7 treatment induces an increase of 11 % of cells in the S-phase. To investigate the potential mechanism underlying the cell cycle arrest Annex V/ PI test was performed, revealing no apoptotic cells in all treatments (D1, I4, I7), in neither U251 nor U87MG cell line at different time points (Supplementary Fig. S3), supporting the hypotheses of a cytostatic rather than cytotoxic effect.

2.3. Wound healing rate closure is inhibited by CFSs from L. lactis D1, I4, and I7 strains

To evaluate the effect of CFSs from L. *lactis* D1, I4, and I7 strains on cell migration and cell-cell interaction, the wound healing assay was performed. As shown in Fig. 3, both U87MG, U251, and T98 cell lines, in the absence of treatment, were able to close the gap within 24 h. In contrast, in the presence of 0.5 mg/mL of all CFSs used, the residual

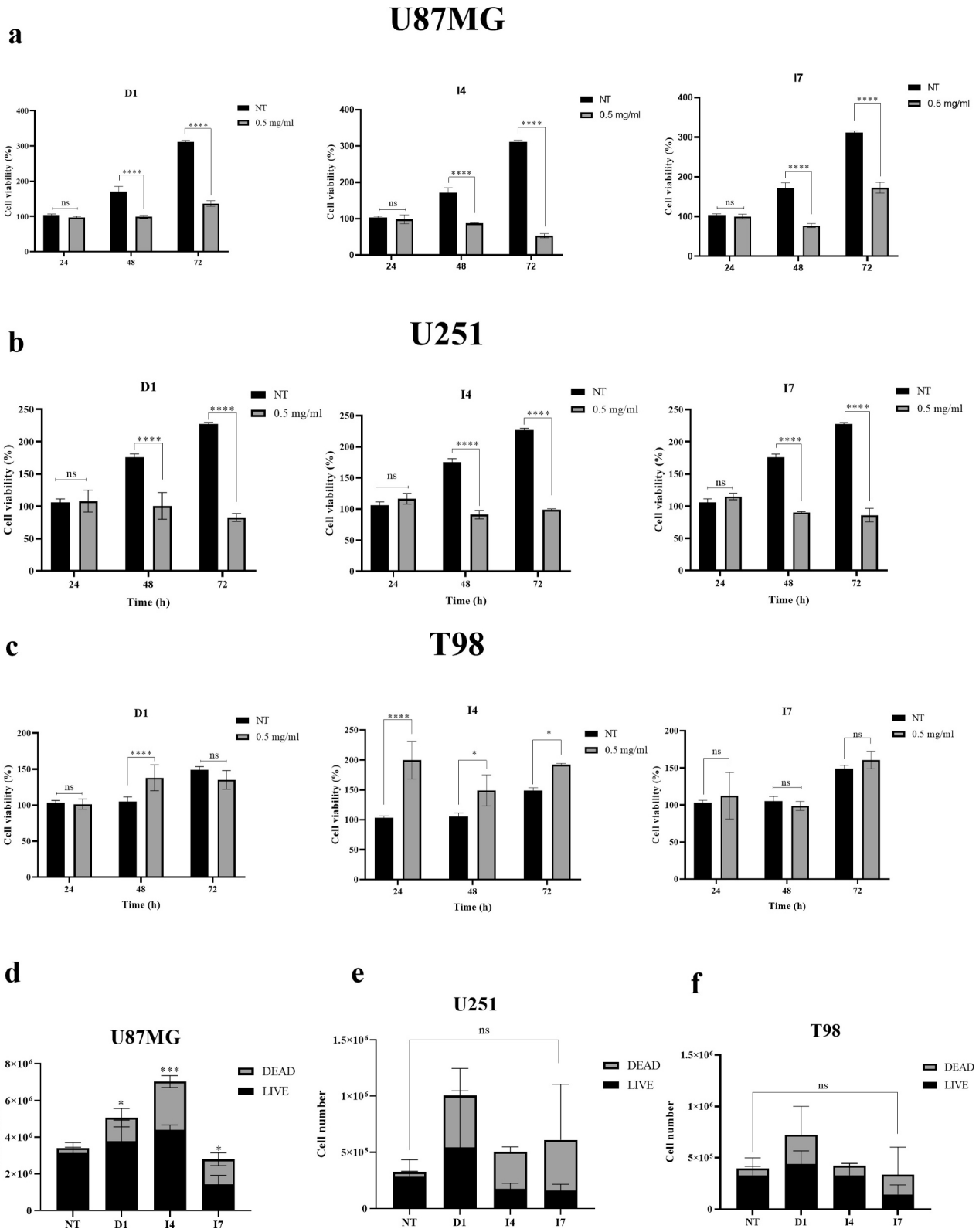

Fig. 1. CFSs from L. ***lactis*** **D1-I4-I7 impair GBM cell viability. (a-b-c)** MTT assay on U87MG (**a**) U251 (**b**) and T98 (**c**) cell lines. Untreated cells (NT) were used as positive control. Error bars are representative of the SD of three independent experiments performed in triplicates. Significance of the data obtained was tested by 2way Anova with Sidak's multiple comparisons (**** $p < 0.0001$, ** $p < 0.05$, *$p = 0.02$ compared to untreated cells; ns: not significant). **(d-e-f)** Trypan blue exclusion assay on U87MG (**d**), U251 (**e**) and T98 (**f**) cell lines. Untreated cells (NT) were used as positive control. Data are presented as mean ± SD of the three independent experiments performed in triplicate ($n = 9$). Significance of the data obtained was tested by Welch's test (*** $p < 0.001$, * $p < 0.05$ compared to untreated cells; ns: not significant). (For interpretation of the references to colour in this figure legend, the reader is referred to the web version of this article.)

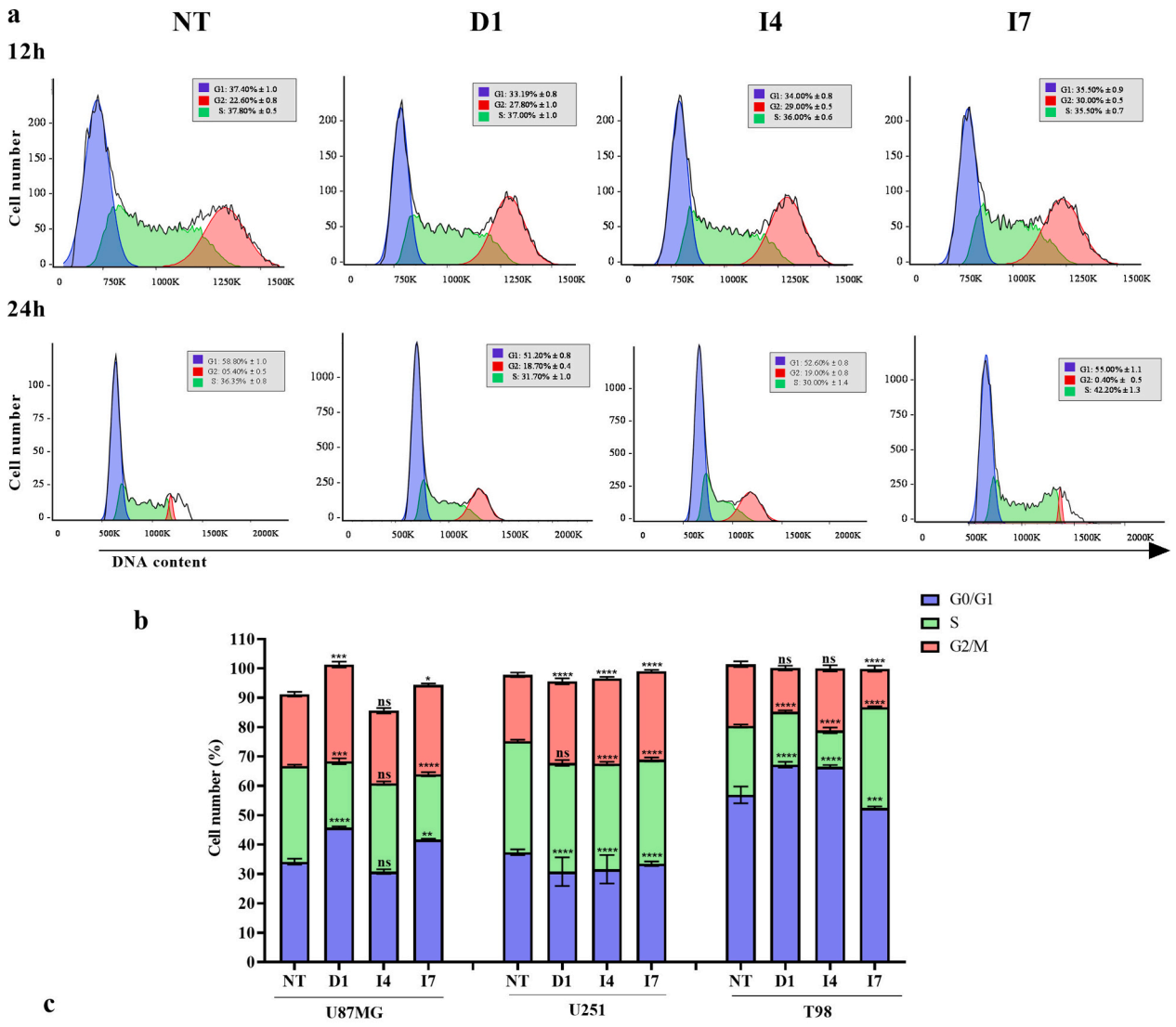

c

U87MG		G1	S	G2
	NT	34.2% ±1.0	32.5% ± 0.5	24.5% ± 0.8
	D1	45.8% ± 0.4	22.6% ± 1.0	32.9% ± 1.0
	I4	30.8% ± 0.8	30.1% ± 0.6	24.7% ± 0.9
	I7	41.7% ± 0.3	22.3% ± 0.7	30.4% ± 0.5
U251		**G1**	**S**	**G2**
	NT	37.4% ±1.0	37.8% ± 0.5	22.6% ± 0.8
	D1	33.2% ± 0.8	37.0% ± 1.0	27.8% ± 1.0
	I4	34.0% ± 0.8	36.0% ± 0.6	29.0% ± 0.5
	I7	33.5% ± 0.8	35.5% ± 0.7	30.0% ± 0.5
T98		**G1**	**S**	**G2**
	NT	55.6% ±0.6	23.4% ± 1.0	21.01% ± 1.0
	D1	67.2% ± 1.0	18.5% ± 0.5	14.9% ± 0.8
	I4	66.5% ± 0.6	12.4% ± 1.0	21.1% ± 1.0
	I7	52.5% ± 0.5	33.4% ± 0.3	13.1% ± 1.0

Fig. 2. CFSs from L. ***lactis*** **D1-I4-I7 impair cell cycle of human glioblastoma cell lines. (a)** Representative Flow cytometry cell cycle analysis of U251 human glioblastoma cell line treated with CFSs from L. *lactis* D1, I4, I7 for the indicated time points. In each panel, boxes show the percentage mean of at least three independent experiments performed in triplicate SD of cells in the different phases of the cell cycle. **(b)** Flow cytometry histogram shows the percentage of cell cycle accumulation during treatments with CFS from L. *lactis* D1, I4, and I7 after 12 h in U87MG, U251, and T98 cell lines. Data are presented as mean ± SD of the three independent experiments performed in triplicate ($n = 9$). Significance of data obtained was tested by the 2way ANOVA with Dunnett's multiple comparisons (**** $p < 0.0001$, *** $p < 0.001$, ** $p < 0.005$, ns: non-significant compared to untreated cells, NT). **(c)** Percentage of U87MG, U251, and T98 treated with CFS of L. *lactis* D1, I4, and I7 for 12 h in the different cell cycle phases.

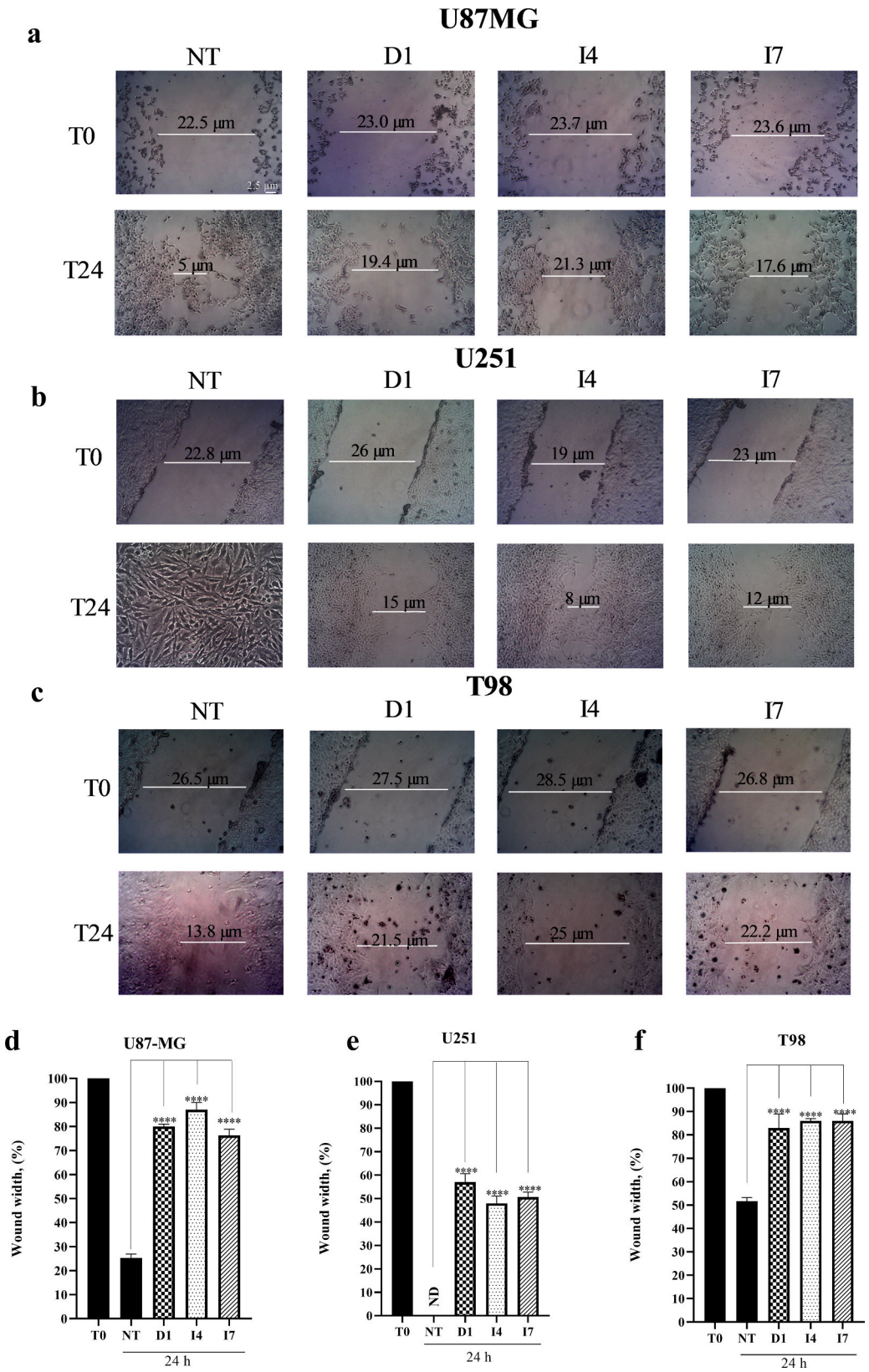

Fig. 3. CFSs from L. ***lactis*** **D1-I4-I7 impair wound healing of human glioblastoma cell lines. (a-b-c)** Representative high-power microphotographs of U87MG (**a**), U251 (**b**), and T98 (**c**) cells treated with 0.5 mg/mL of CFSs. Images were taken at time 0 (T0) and 24 h (T24) after CFSs treatment (10× total magnification, scale bar, 2.5 µm). T0 represents the wound width at the moment of the scratch. Arbitrary arrows pointing the wound edges were drawn on the T0 image and applied to each sample's single photograms after 24 h. The average margin distance was measured at five points and the results were expressed as a percentage of residual wound width at T24 compared to T0 of the same sample. **(c-e)** Quantitative analysis of the migration rate tested on U87MG **(d)**, U251 **(e)**, and T98 **(f)**. Data are presented as mean ± SD of the three independent experiments performed in triplicate ($n = 9$). The significance of data obtained was tested by the Ordinary One-way ANOVA with Sidak's multiple comparisons (**** $p < 0.0001$, compared to non-treated cells, NT; ND: not detected).

space was significantly higher compared to control conditions. In particular, in the presence of 0.5 mg/mL of CFSs, the residual space was 80 %, 87 %, and 76 % in treated U87MG (Fig. 3d), 57 %, 48 %, and 50 % in treated U251 (Fig. 3e), and 83 %, 86 %, and 86 % in treated T98 (Fig. 3f), from *L. lactis* D1, I4, and I7 strains respectively. These data indicate inhibition of wound closure induced by the preincubation with the postbiotics produced by L. *lactis* D1, I4, and I7 strains, suggesting an inhibitory effect on proliferation, migration, or both.

2.4. Cell migration of GBM cell lines is inhibited by CFS of L. lactis I4 and I7, but not D1

To further investigate the effects of CFSs on cell migration of U87MG, U251, and T98 cells, a chemotactic assay in Transwell Plate 8 μm Pore Size in the presence of 0.5 mg/mL of CFSs was performed. Migration of untreated cells was used as positive control. No significant difference was observed in the migration of cells treated with 0.5 mg/mL of CSF from L. *lactis* D1 strain in all three cell lines, suggesting an inhibitory effect on proliferation, but not on migration. In contrast, treatment with 0.5 mg/mL of CFSs from L. *lactis* I4 and I7 strains reduced migration ability (Fig. 4d-f). In particular, CFS from L. *lactis* I4 exhibits a stronger inhibitory effect on U87MG cell migration (Fig. 4d) compared to the other cell lines, whereas the CFS from L. *lactis* I7 predominantly inhibits the migration of T98 cells (Fig. 4f). In the case of U251 cells, both CFSs (I4 and I7) appear to have a comparable effect (4e). This may suggest that the inhibition of migration by these extracts may occur in a specific and selective manner.

2.5. CFSs from L. lactis D1, I4, and I7 strains inhibit spheroid growth over time

Recently, multicellular tumour spheroids have been used to track the evolution of GBM, elucidate resistance mechanisms, and propose novel therapy strategies (Alves, Calori, Bi, & Antonio Claudio, 2023). Here, we induced spheroids formation of U87MG cells by self-aggregation of cells in the bottoms of non-adherent round bottom 96-well plates. Once formed, spheroids were treated with 0.5 mg/mL of each CFSs under study and observed daily. Spheres diameter was measured from 24 h to 6 days after treatments. As shown in Fig. 5a, untreated spheroids appear tighter and denser over time. Meanwhile, after 6 days, the spheroid structure was totally disintegrated when treated with postbiotics, showing a loose and uneven cell aggregate. Furthermore, the treated samples showed a much larger cell distribution area than the untreated ones. Representative images of spheroids with and without postbiotics

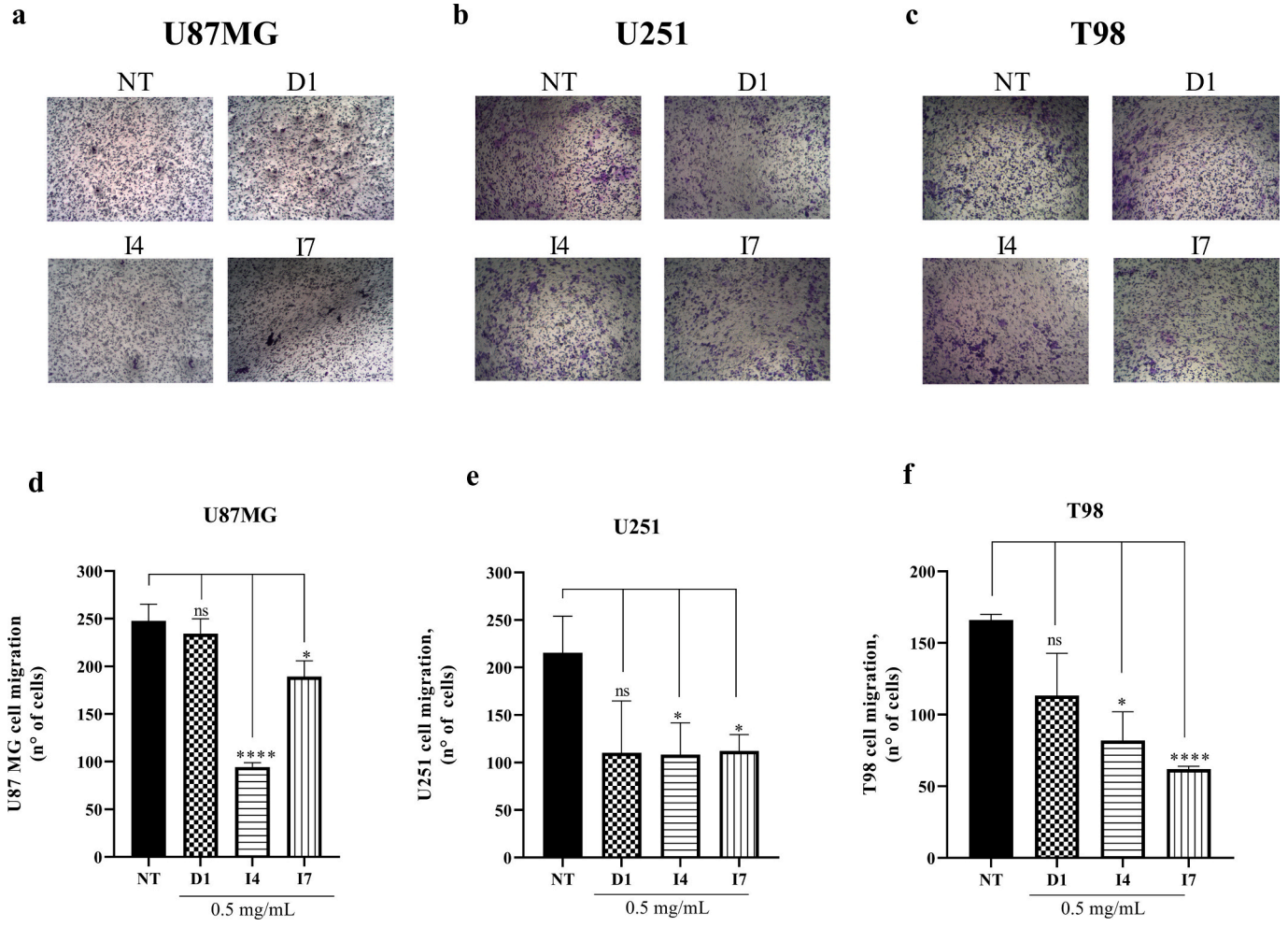

Fig. 4. CFSs from L. ***lactis*** **D1-I4-I7 impair migration of human glioblastoma cell lines.** Cells were plated in serum-free media and allowed to migrate for 4 h at 37 °C towards DMEM 5 % FBS. At the end of the assay, the cells on the lower filter surface were fixed, stained, and counted as described in Materials and Methods. **(a-b-c)** Representative high-power microphotographs of U87MG (**a**), U251 (**b**), and T98 (**c**) cells treated with 0.5 mg/mL of CFSs. Cells were observed microscopically under an inverted microscope (4× total magnification) and counted (at 10× total magnification) in at least three randomly selected visual fields. Number of migrated cells was calculated using ImageJ software. **(d-e-f)** Number of migrated cells of U87MG (**d**), U251 (**e**), and T98 (**f**) cells. Untreated (NT) cells were taken as positive control. Data are presented as mean ± SD of the three independent experiments performed in triplicate ($n = 9$). Significance of the data obtained was tested by Welch's test (**** $p < 0.0001$, * $p = 0.02$, compared to untreated cells; ns: not significant).

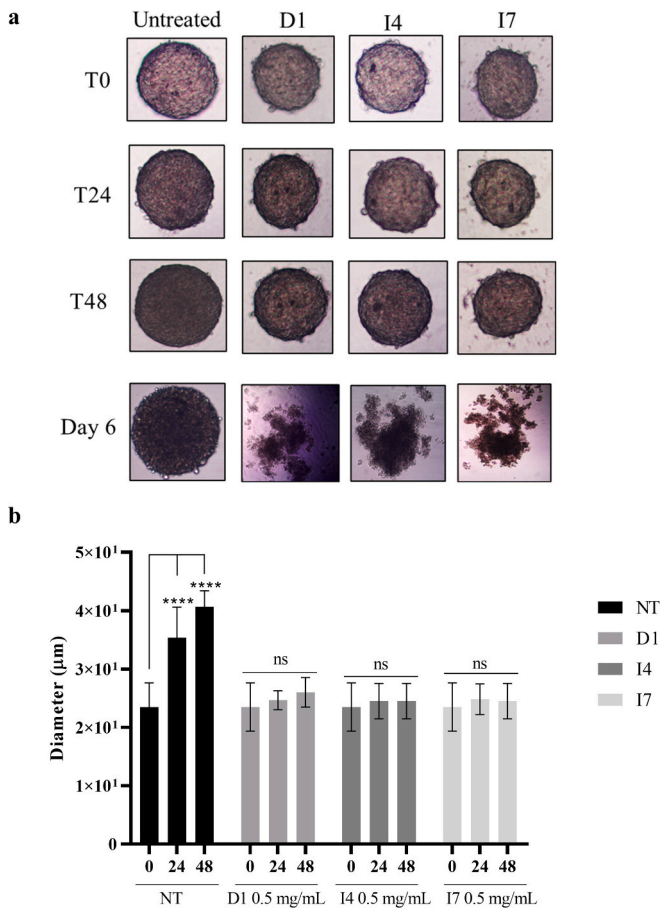

Fig. 5. CFSs from *L. lactis* D1-I4-I7 impair spheroid formation of the human glioblastoma cell line U87MG. Cells were plated and allowed to form spheroids. Following spheres formation, 0.5 mg/mL of the tested postbiotics were added. (**a**) Representative photographs of spheroids with and without postbiotics. Pictures were taken from 24 h up to 6 days after treatments (10× total magnification, scale bar: 2.5 µm). (**b**) Quantifications of spheroid diameter in the absence (NT) and presence of postbiotics (D1, I4, I7). Data are presented as mean ± SD of the three independent experiments performed in triplicate, each experiment included six replicates per sample ($n = 18$). Significance of data obtained was tested by the 2way Anova with Sidak's multiple comparisons (**** $p < 0.0001$, compared to spheroid diameter at time 0; ns: not significant).

are shown in Fig. 5a. Overall, postbiotics exposure inhibits spheroid growth over time, whereas the diameter of non-treated spheroids continues to grow (Fig. 5b).

2.6. CFSs from L. lactis strains do not affect the integrity of the blood-brain-barrier nor astrocytes viability

To better elucidate the effects of these CFSs on healthy non-proliferating cells and on the blood-brain barrier, we established an *in vitro* co-culture model as previously described in detail (Nielsen et al., 2017). In particular, in a Transwell setup, primary porcine brain endothelial cells (pBECs) were seeded on semipermeable membranes pre-coated with proteins of the basement membrane (fibronectin and collagen IV), and astrocytes cultured in the bottom compartment as a non-contact co-culture (Fig. 6a). The astrocytes are part of the blood-brain barrier and secrete stimulating factors that are essential for maturation and maintenance of the brain endothelial cells in order to be tight, polarised, and have a functional vesicular subcellular transport system (Toth et al., 2018). Following barrier induction with differentiation factors, the barrier integrity was validated by immunofluorescence analysis of the tight junction proteins claudin 5, ZO-1, and adherens junction protein p120 catenin. Our results demonstrate no significant alteration in the expression and in the localization of the endothelial barrier proteins, showing *in vivo*-like paracellular localization (Fig. 6c-d-e). Integrity and permeability of the *in vitro* BBB model system were also evaluated by Trans Endothelial Electrical Resistance (TEER) (Waithe, Peng, Childs, & Tharakan, 2024), measured over time (1, 6, and 24 h) after the treatment with CFSs (Fig. 6b). Replacement of medium in the *in vitro* BBB models is expected to introduce an immediate drop in TEER values and the drop after media change and inclusion (Fig. 6b) has been therefore observed. However, the fact that the TEER drop does not fall below 300–400 $\Omega \cdot cm^2$, coupled with the rapid increase observed in the following hours, suggests that tight junctions remain intact at a level that prevents paracellular transport of small molecules (Nielsen et al., 2017). Imaging of tight junctions and TEER measurements confirm that none of the three selected CFSs impair the blood-brain barrier integrity. Moreover, future studies will be aimed at identifying the active molecules within the CFSs, and at comparing their effect to those compounds known to impair BBB function. Finally, to test the cytotoxicity and specificity of these CFSs, in a separate experimental setting, a Trypan blue exclusion test was performed on differentiated primary astrocytes. Untreated astrocytes were used as a positive control. CFSs of L. *lactis* D1, I4, and I7 did not affect the viability of astrocytes, demonstrating a selective effect only on proliferating undifferentiated cells (Fig. 7).

3. Discussion

This study represents the first investigation into the effects of cell-free supernatants (CFSs) from three distinct *Lactococcus lactis* subsp. *lactis* strains (D1, I4, and I7), isolated from natural whey culture, on *in vitro* glioblastoma models. We evaluated their impact on key cancer hallmarks, including proliferation, migration, and spheroid formation, using U87MG, U251, and T98 glioblastoma cell lines. Despite their common glioblastoma origin, these cell lines exhibit distinct biological features. Indeed, it is well known that U87MG cells proliferate and migrate faster than the others under the same culturing conditions, while U251 cell line has an up-regulated glycolysis pathway, resulting from the "Warburg effect" that is associated with several cancer cell properties such as adaptation to low nutrient conditions and resistance to oxidative stress and apoptotic stimuli (Li et al., 2017). Moreover, T98 cell lines overexpress MRPs (multidrug resistance proteins) and BCRP (breast cancer resistance protein) that pump out various anticancer agents, conferring them multidrug resistance (Nakatsuma et al., 2010). All the experiments reported in this study were performed on the three cell lines, showing similar effects and suggesting that CFSs are able to affect different molecular mechanisms underlying all the cancer hallmarks that make GBM difficult to treat. A preliminary screening was performed to evaluate the effect of the CFSs from eight L. *lactis* different strains, on the proliferation of the U87MG cell line (De Chiara et al., 2024). Results showed that all postbiotics tested can affect cell viability in a time- and dose-dependent manner. However, based on our previous results concerning probiotic properties (De Chiara et al., 2024), A3, A5, I4, and I7 *L. lactis* strains exhibited pronounced probiotic properties in terms of survival under simulated gastrointestinal stress and competitive exclusion with pathogens, compared to all other strains tested. Nevertheless, based on the MTT assay on U87MG cells, CFSs from A3 and A5 demonstrated a cytotoxic rather than a cytostatic effect. For these reasons, postbiotics from A3 and A5 were excluded, and CFS from D1 strain, together with I4 and I7, were selected for further analysis since they exhibited a less toxic effect at a concentration of 0.5 mg/ml. Although these findings highlight the potential biological activity of selected CFSs, the therapeutic window and safety margins will be fully investigated on the active fraction. These selected CFSs were further tested on the cell viability of U251 and T98 cells as well. In particular, CFSs of L. *lactis* D1, I4, and I7 decreased cell viability of both U87MG and U251 after 48 and 72 h, but no effects were detected after 24 h. Contrariwise, CFSs of D1, I4, and I7 strains did not affect T98 cells, as they seemed to increase the

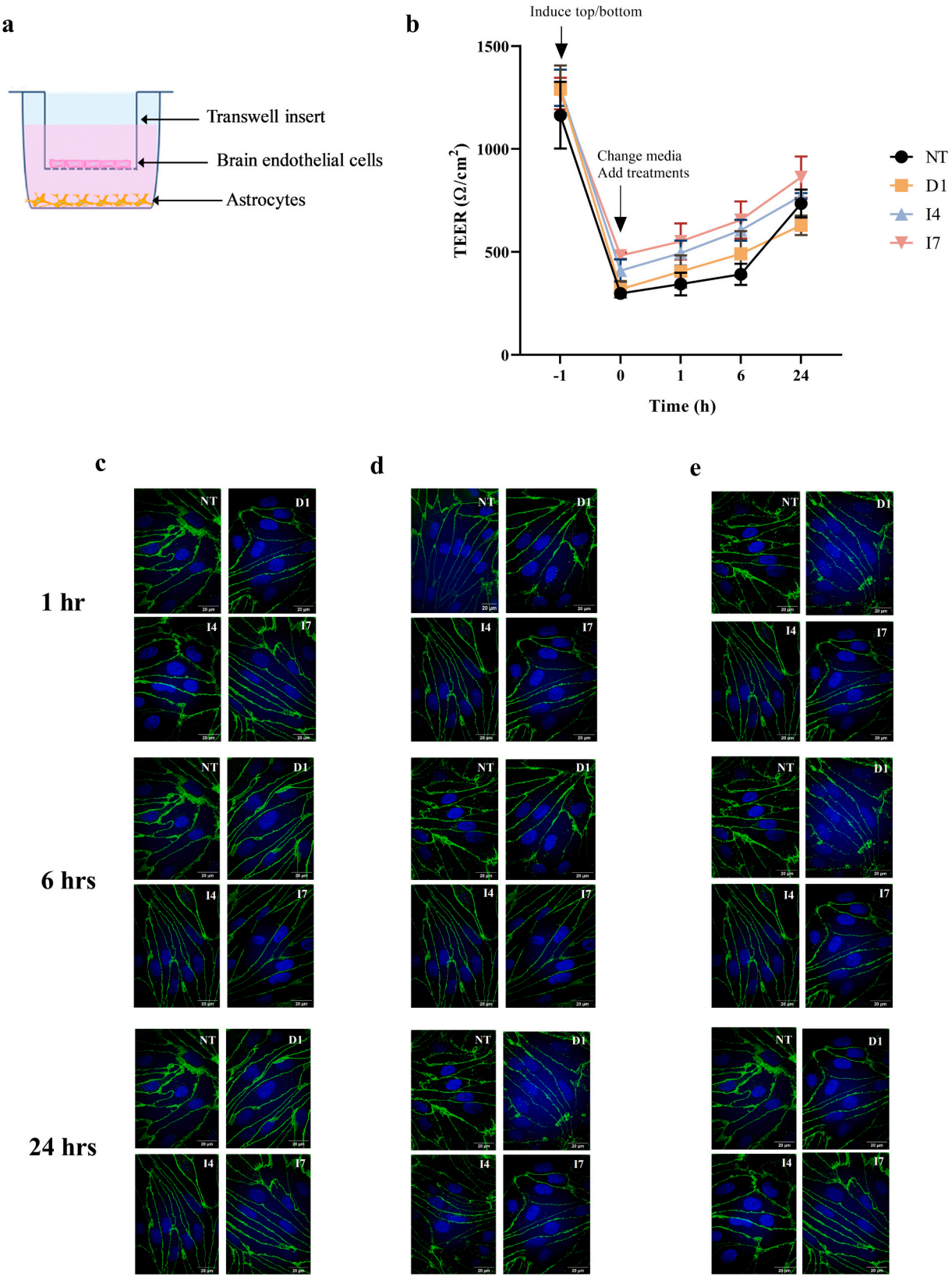

Fig. 6. CFSs from *L. lactis* D1-I4-I7 do not affect BBB integrity in an *in vitro* model. (**a**) Schematic illustration of the applied non-contact co-culture (NCC) blood-brain barrier (BBB) model setup, including pBECs and astrocytes. (**b**) Validation of the barrier integrity by transendothelial electrical resistance (TEER) (Ω/cm2) presented as mean values (±SEM) of the three independent experiments performed in triplicate (n = 9), and X axis marking the hours of barrier inducement ($T = -1$) and the hours of probiotics' treatments. (**c-e**) Confocal microscopic imaging with 60× magnification of immunofluorescence staining visualizing the adherens junction (AJ) proteins (red) p120 catenin (c), and the tight junction proteins (TJ) claudin 5 (d), and ZO-1 (e). In blue the Hoechst stain of nuclei. Scale bar equal to 20 μm. (For interpretation of the references to colour in this figure legend, the reader is referred to the web version of this article.)

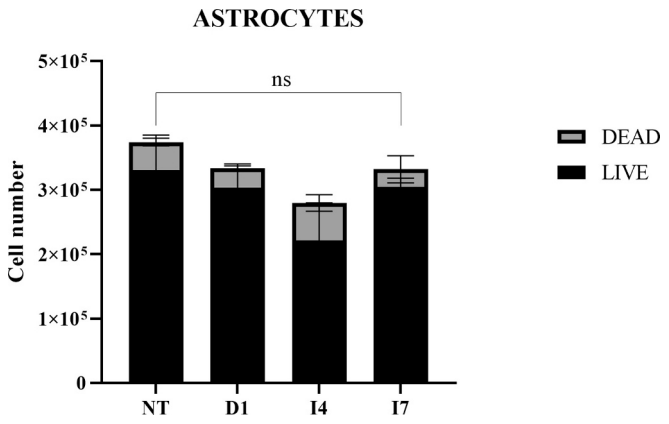

Fig. 7. CFSs from *L. lactis* D1-I4-I7 do not affect cell viability of healthy astrocytes. Trypan blue exclusion assay. Untreated cells (N.T.) were used as positive control. None of the three selected postbiotics alters astrocyte viability Data are presented as mean ± SD of the three independent experiments performed in triplicate (n = 9). Significance of the data obtained was tested by Welch's test (*** $p < 0.001$, * $p < 0.05$ compared to untreated cells; ns: not significant). (For interpretation of the references to colour in this figure legend, the reader is referred to the web version of this article.)

cell viability. This resistance in T98 cells could be due to the upregulation of efflux transporters (Bhatia et al., 2012) and/or enhanced DNA repair mechanisms (Erasimus, Gobin, Niclou, & Van Dyck, 2016), which could mitigate the cytostatic effects of the CFSs. It is well recognized that each glioblastoma cell line harbours distinct genetic, epigenetic, and metabolic profiles that can influence its response to external stimuli or treatments (Pagano et al., 2024). The increased viability or resistance observed in the T98 cell line following CFS treatment could indeed reflect such intrinsic differences. In particular, T98G cells are known to carry mutations in TP53 and unmethylated MGMT, thus displaying a relatively resistant phenotype compared to other glioblastoma models due to the DNA repair activity (Lanskikh et al., 2024). This variability in response highlights the importance of considering inter- and intra-tumoral heterogeneity when evaluating the biological effects of microbial-derived products. Such differences may provide valuable insights for the development of personalized therapeutic strategies, where the molecular and genetic background of the tumour dictates its susceptibility to specific bioactive compounds. Moreover, the observed heterogeneity may also mirror the diverse metabolic and signalling interactions between tumour cells and microbial components, highlighting the need to explore how microbial variability could be harnessed or modulated to optimize therapeutic efficacy across distinct glioblastoma subtypes.

It is also important to consider that MTT assay can be limiting, despite its continued use for assessing cell viability. This assay measures the activity of succinate dehydrogenase, a mitochondrial enzyme involved in the Krebs cycle and ATP production. However, in cells undergoing imminent death, this enzyme's activity can appear upregulated, as mitochondria may release more enzymes. As a result, the MTT assay, in some cases, may not accurately reflect true cell viability, since increased mitochondrial activity could indicate a cell's attempt to sustain function prior to death, rather than actual cell health. This limitation can affect the interpretation of results, particularly in stressed or damaged cells (Ghasemi, Turnbull, Sebastian, & Kempson, 2021). Trypan blue exclusion assay supports the observation that these CFSs are able to impair cell viability.

The anticarcinogenic effect of microbial metabolites may be due to different mechanisms, including induction of apoptosis, and/or inhibition of cell proliferation (Kvakova, Kamlarova, Stofilova, Benetinova, & Bertkova, 2022; Wu, Zhang, Ye, & Wang, 2021). PI-staining flow cytometry analysis was performed to investigate whether L. *lactis* D1, I4, and I7 CFSs may impair cell proliferation through cell cycle arrest. U87MG, U251, and T98 cells treated with these supernatants showed an accumulation in G1 or G2/M phase compared to the untreated control. The only exception was represented by I7 CFS, which induces an increase of T98 cells in S-phase. This accumulation may result from forced entry into the S-phase, causing cells to initiate DNA replication prematurely. Consequently, the replication fork encounters replication stress, leading to the arrest of T98 cells in S-phase, likely due to the activation of the intra-S-phase checkpoint. In addition, Annex V/ PI staining demonstrates that none of the selected postbiotics induced apoptosis, suggesting that CFSs inhibit proliferation in a cytostatic manner without killing tumour cells. Inhibition of proliferation of tumour cells without inducing cell death could potentially reduce cytotoxicity to normal, non-tumour host cells, particularly if those normal tissues are low- or non-proliferating, as in the case of central nervous system cells (Morley, Ferguson, & Koropatnick, 2007). Indeed, data reported in this study show that none of the CFSs under investigation is able to affect the viability of primary astrocytes, the differentiated healthy counterpart of GBM cells. Tumour progression is dependent on the ability of cells to migrate and invade, infiltrating adjacent tissues (Fares, Fares, Khachfe, Salhab, & Fares, 2020). The wound healing assay is a technique used to study cell migration and cell-cell interaction. It is specifically a 2D cell migration approach to semi-quantitatively measure cell migration of a sheet of cells. Our results show that non-treated cells migrate towards the wound, thereby closing the wounded edges. In contrast, treatment with CFSs from the three probiotics under study significantly decreases the wound healing rate and closure in all the tested GBM cell lines. To further investigate the inhibition of cell migration properties of microbial metabolites, a Transwell migration assay was also performed. Indeed, these two experimental approaches involve distinct assays. The wound healing assay is a 2D migration method that is useful for investigating cell-cell interactions, where cells adhere to a polystyrene surface. In this case, the inhibitor's effect may be more related to proliferation rather than migration. The transwell assay is used to study directional migration towards a chemoattractant and typically separates migration from proliferation, as the cells are not allowed to proliferate. FBS-directional cell migration was inhibited by I4 and I7, but not D1, suggesting that the latter influences proliferation but not migration. Moreover, CFSs from I4 and I7 appear to have different behaviours depending on the treated cell type. These findings suggest that CFSs exert differential effects based on strain-specific metabolic profiles. The inhibition of migration may be linked to alterations in cytoskeletal dynamics or extracellular matrix remodelling. Future studies should explore whether these postbiotics influence metalloproteases (MMPs) activity or integrin signalling, which are critical regulators of glioblastoma cell motility.

2D individual cell-tracking experiments and Transwell assays cover different phenotypes and hallmarks of cell motility and adhesion (Pijuan et al., 2019), providing orthogonal information that can be used collectively to better describe the biological effects of CFSs on GBM cancer cells. However, the main drawback in anticancer therapy development is the use of 2D cultures *in vitro* models. On this issue, here we developed a 3D cell culture models that resemble tumour tissues by reproducing the *in vivo* complex architecture more faithfully. The phenotypic changes observed during exposure to postbiotics released by L. *lactis* strains can be used as a measure of their efficacy. Here, for the first time, we assessed the effect of L. *lactis* postbiotics on spheroid structures and growth, demonstrating that all the CFSs under study can inhibit spheroid growth and induce their disaggregation when added to the culture media. The establishment of tumour spheroids significantly increased the opportunity to investigate anti-cancer agents *in vitro* since spheroids represent the best mimics of solid tumors *in vivo* as they exhibit cellular heterogeneity, diffusion-limited distribution of oxygen and nutrients, cell-cell signalling, growth kinetics, cell-cell interactions, and therapeutic resistance to treatment modalities. Taken together, our results suggest that metabolites produced by L. *lactis* D1 are able to inhibit cell proliferation but not migration, whereas metabolites

produced by L. *lactis* I4 and I7 are able to inhibit cell proliferation as well as cell migration. No one is able to induce cell death, but they all impair 3D cell spheroid growth. One possibility is that secreted bacterial metabolites interfere with intercellular adhesion molecules, which are important for migration and invasion, or hypoxia-related signalling, crucial for spheroid maintenance.

One of the major challenges in cancer treatment is selectivity, namely, the ability of potential therapeutic agents to distinguish between malignant tumour cells and healthy ones represented by neurons, astrocytes, and endothelial cells of the blood-brain barrier (BBB) (Abbott, Patabendige, Dolman, Yusof, & Begley, 2010). Indeed, some chemotherapy might lead to the development of central neurotoxicity, due to neuroinflammation, neuroendocrine changes, and alterations in the BBB that allow increased access of cytotoxic agents and pro-inflammatory cytokines to neurons and supportive glial (astrocytes and microglia) cells, as well as secondary activation of glial cells and myelin-producing (oligodendrocyte lineage) cell defects (Was et al., 2022). To better investigate the effects of CFSs, here we established an *in vitro* model of BBB and showed that CFSs do not affect endothelial cell viability nor BBB integrity, demonstrating once again that these compounds are safe for non-proliferating-differentiated healthy cells and their effects are exerted only on proliferating undifferentiated cancer cells. Moreover, the presence of the BBB reduces the effectiveness of anticancer therapy for human GBM. Endothelial cells of microvessels and capillaries of the brain, connected by tight contacts, limit the intercellular transport of hydrophilic drugs with a molecular weight > 500 Da (Pandit, Chen, & Götz, 2020). The presence in CFSs of lipophilic compounds such as liposoluble vitamins, short-chain fatty acids, neurotransmitters, and other organic acids suggests that, at least partially, these substances could bypass the BBB hindrance and easily reach tumour cells (Hoyles et al., 2018). Therefore, ongoing studies by HPLC and highly sensitive MS methods in our lab are aimed at evaluating the CFSs passage through the BBB and at individual screenings with purified fractions that will allow us to determine if the observed effects are caused by a single compound or by a synergistic effect.

In conclusion, our *in vitro* study demonstrates for the first time that postbiotics from L. *lactis* strains D1, I4, and I7 possess promising anticancer properties by selectively inhibiting glioblastoma cell proliferation, migration, and spheroid growth without affecting healthy cells, such as astrocytes and endothelial cells, or BBB integrity. These findings offer a complementary perspective to standard therapies such as Temozolomide, which, while effective, can be associated with systemic toxicity and limited selectivity. The selective activity observed for the CFSs provides a valuable basis for further investigation, particularly to assess how these postbiotics might interact with Temozolomide. Testing the combined effects will be important to explore potential synergistic interactions, to better understand differential cellular responses, and to establish whether the CFSs could modulate or enhance the activity of conventional treatments in a controlled and systematic manner. Future studies will focus on identifying specific bioactive molecules responsible for these effects and elucidating their mechanisms of action. Additionally, *in vivo* validation will be essential to assess therapeutic potential and optimize delivery strategies for glioblastoma treatment. These findings pave the way for exploring LAB-derived fermented foods as a natural source of bioactive compounds with potential applications in cancer therapy.

4. Materials and methods

4.1. Bacterial strains, media, and growth conditions

Lactococcus lactis subsp. *lactis* strains (A3, A5, B1, D1, D3, I1, I4, I7), used in the study, were previously isolated from natural whey starter cultures. Their different RAPD (Random Amplification of Polymorphic DNA) profiles and probiotic characteristics were previously described (De Chiara et al., 2024; Marasco, Gazzillo, Campolattano, Sacco, & Muscariello, 2022). *Lactococcus* strains were grown at 30 °C in ESTY broth supplemented with lactose 1 % (*w/v*). Medium was supplied from Condalab (Madrid, Spain).

4.2. Postbiotic production

L. lactis strains were cultured on ESTY broth overnight and then subcultured in 100 mL of the same fresh medium. Absorbance was measured periodically at 600 nm until reached 1 OD. To separate supernatants from bacterial pellets, media were centrifuged at 3750 rpm, 30 min, 4 °C. Supernatant samples were sterilized using a 0.22 μm pore size filter and neutralized (pH 7.00) with NaOH 1 M. Cell-free supernatant (CFS) was stored at −80 °C and then lyophilized (VirTis SP Scientific Wizard 2.0). Dried CFSs were resuspended in Dulbecco's Modified Eagle Medium (DMEM, Life Technologies, Paisley, UK).

4.3. Cell culture

Human glioblastoma cell lines U87MG, U251, and T98 were cultured in DMEM (Dulbecco's Modified Eagle Medium) containing 10 % fetal bovine serum (FBS, Life Technologies, Paisley, UK). 100 U/mL of penicillin/streptomycin was added to the culture media. Cells were incubated at 37 °C in a humidified atmosphere containing 5 % CO_2, and 95 % atmospheric air. Astrocytes purified from 1 to 2 days old Sprague–Dawley rats were used as a control of healthy cells and were grown in DMEM low glucose supplemented with 10 % FBS and 100 U/mL of penicillin/streptomycin for 3 weeks in a humidified incubator at 37 °C, 5 % of CO_2, 95 % atmospheric air.

4.4. Cell viability assay

Cell viability in response to treatment with CFSs, was assessed either by Trypan blue exclusion test or by thiazolyl blue tetrazolium bromide (MTT) assay as previously described with some modification (Sharma et al., 2018; Della Valle et al., 2022). For the MTT assay, an initial screening was performed on U87MG cells, testing all the lyophilized CFSs of all the L. *lactis* strains, solved in DMEM media in desirable concentrations (50, 5, 0.5 mg/mL). Subsequently, three CFSs (*L. lactis* D1, I4, I7) were selected, and a single concentration (0.5 mg/mL) was chosen for further testing on U87MG, U251, and T98 cell lines. Briefly, 2.5×10^3 U87MG, 5×10^3 U251, and 5×10^3 T98 cells/well were grown in 96-well plates for 24 h and then treated with 0.5 mg/mL of CFSs. Concomitantly, cells without treatments were used as a positive control. 10 μL of the 5 mg/mL MTT solution in PBS, (Invitrogen-Life Technologies, Eugene, OR, USA) were added to wells, and incubated for 3 h at 37 °C. After incubation, 100 μL of stop solution were added to each well. Then, the optical densities were measured at 595 nm using the Microplate Reader (GLO Max Discovery, Promega). The cell viability rate was assessed after 24, 48 and 72 h and calculated as follows:

cell metabolic activity rate (%) = (OD treated) / (OD control) x 100.

For the Trypan blue exclusion test, 2.5×10^3 U87MG, U251, and T98 cells were grown and then treated with 0.5 mg/mL of three selected CFSs. Cells were then incubated at 37 °C in a humidified atmosphere containing 5 % CO_2 for 24 h. Then, the cells were detached, stained with a 0.4 % (*w/v*) Trypan blue solution, counted using a Burker chamber, and reported as the number of live/dead cells.

4.5. Cell cycle analysis and apoptosis assay

Cell cycle analysis was performed by Fluorescence-Activated Cell Sorting (FACS) as previously described (Cito et al., 2015; Di Zazzo et al., 2014). Briefly, U87MG, U251, and T98 cells were treated with 5.0 mg/mL of D1 and I4, and 0.5 mg/mL of I7 CFS, after synchronization with 1 % FBS for 12 h, and then treated for 12 and/or 24 h at 37 °C. The cells were then washed twice with phosphate-buffered saline (PBS), fixed with EtOH 70 %, permeabilized with Triton 0.1 % and finally stained in

10 μg/mL of propidium iodide (PI) with 5 μg/mL RNase in the dark at 4 °C overnight. Apoptotic cells were detected by annexin V-FITC/PI staining assay following the manufacturer's instructions as previously described (Boccellino et al., 2021) (A432; Leinco Technologies, Inc.). Briefly, the cells were treated with 5 mg/mL of D1 and I4 and 0.5 mg/mL of I7 CFS, after synchronization with 1 % FBS for 12 h, and incubated for 24–48 h, washed twice with annexin V-binding buffer and resuspended in 1 ml of the same buffer (1×10^6). Fifteen minutes before flow cytometry analysis, 5 μl of PI and 5 μl di Annexin-V-FITC were added to 100 μl of each sample and then analysed by Accuri C6 Flow Cytometer (Becton Dickinson, Franklin Lakes, NJ, USA). As a control of efficacy of materials and Annex V/ PI test reagent, NIH3T3 cell line were treated with Cisplatin 60 μM, which induces cell death *via* an apoptotic pathway in a time-dependent manner (see Supplementary Fig. S4). Fluorescence was determined by Accuri C6 Flow Cytometer (Becton Dickinson, Franklin Lakes, NJ, USA). All cells were acquired with threshold on FCS-H 80,000 and gated in FSC-A/SSC-A dot plot as represented in Fig. S5(a-c). Since when single cells in the flow cell pass through the BD Accury-C6 laser beam, their FSC-A and FSC-H signals correlate linearly and plot along a relatively straight line, single cells were gated by plotting FSC-A against FSC-H as shown in Fig. S5d. At least 15,000 total events were acquired, of which 5000 events were PI positive and analysed. Data were analysed with Floreada.io online software or Flowjo10.4 software.

Wound healing assay.

The wound healing assay or scratch test was performed as previously described (Gentile, Pastorino, Bifulco, & Colucci-D'Amato, 2019). Briefly, 6×10^3 U87MG, U251, and T98 cells were seeded and grown to confluence in DMEM/10 % FBS for 24 h. Afterwards, the cell monolayers were wounded with a yellow tip and concomitantly treated with 0.5 mg/mL of each CFS. Untreated cells were used as a positive control. Images were taken immediately after scratch formation (T0) and after 24 h by using an inverted microscope (Nikon Eclipse TE300, NIKON INSTRUMENTS INC.), equipped with the AmScope 3.7 Software. To quantify the wound healing rate, arbitrary arrows pointing the wound edges were drawn on the T0 image and were further applied to the single photograms of each sample after 24 h. The average margin distance was measured at five points and the results were expressed as a percentage of residual wound width at T24 compared to T0 of the same sample.

4.6. Transwell migration assay

The migration assay (Zhou et al., 2019) was performed using Transwell Plate 8 μm Pore Size (Sarstedt, Darmstadt, Germany). Briefly, 7×10^5 U87MG, 4×10^4 U251, and 4×10^4 T98 cells treated and untreated with 0.5 mg/mL of CFS, were plated on serum-free media and allowed to migrate for 4 h at 37 °C towards DMEM 5 % FBS. At the end of the assay, cells in the upper chamber were removed using cotton swabs, while cells on the lower filter surface were fixed in cold MetOH 100 % for 15 min, stained with 0.05 % crystal violet for 30 min at room temperature, and then washed with tap water. Migrated cells were counted under an inverted microscope (Nikon Eclipse TE300, NIKON INSTRUMENTS INC.) in at least three randomly selected fields at 10× magnification. The number of migrating cells was calculated using ImageJ software.

4.7. Tumour spheroid

U87MG spheroids were formed by self-aggregation of cells in the bottoms of non-adherent round bottom 96-well plates (Bioflat, Sarstedt, Numbrecht, Germany), by following the method of Sivakumar, with some modifications (Sivakumar, Devarasetty, Kram, Strowd, & Skardal, 2020). Briefly, 100 to 500 cells in 100 μL of media were pipetted into individual wells and allowed to form cell-cell connections over the course of 24 h. Once the sphere was formed, 0.5 mg/mL of tested postbiotics were added. Pictures were taken after 0, 24 and 48 h and checked every day for 6 days of treatments by using an inverted microscope (Nikon Eclipse TE300, NIKON INSTRUMENTS INC.). Single sphere diameter was measured with the AmScope 3.7 Software.

4.8. In vitro study on the blood-brain barrier (BBB)

4.8.1. Animals

All animals used in the study have been treated according to relevant ethical guidelines. This includes that methods are reported in accordance with ARRIVE guidelines (https://arriveguidelines.org), on the ethical use of animals (European Communities Council Directive of 24 November 1986; 86/609/ECC), and Danish guidelines.

Porcine brains were obtained as byproducts of the Danish food industry. Danish Slaughterhouses are under strict supervision and observation by the Danish Ministry of Environment and Food. According to the "Danish Crown" the pigs are anesthetized with 80–90 % CO_2 and then terminated by cutting their carotid artery.

Rats used for isolation of astrocytes were bred and group-housed in the local animal facility at an ambient temperature of 22 °C–23 °C and on a 12/12 h dark/light cycle under the inspection of the veterinarian and according to Danish regulations for lab animals. The rats were euthanized with the CO_2 method before they were sacrificed in accordance with international guidelines on the ethical use of animals (European Communities Council Directive of 24 November 1986; 86/609/EEC) and Danish guidelines. No *in vivo* experiments on animals or human material were used in these experiments.

4.8.2. Cell cultures and an in vitro BBB model establishment

Astrocytes were purified from 1 to 2 days old Sprague–Dawley rats and brain microcapillaries were purified from 5 to 6 months old pigs. Selective cultures of porcine brain endothelial cells (pBECs) were established in a non-contact co-culture (NCC) *in vitro* BBB model as described(Nielsen et al., 2017). Following primary cell purifications, astrocytes were cultured in poly-L-Lysine pre-coated 12-well plates in low glucose DMEM supplemented with 10 % fetal bovine serum (FBS), penicillin (100 U/mL), and streptomycin (100 μg/ml) for three weeks before NCC establishment. Porcine brain microcapillaries were seeded on type IV collagen- (150 μg/mL) and fibronectin (50 μg/ mL) coated T75 flasks using DMEM-F12 supplemented with 10 % plasma-derived serum (PDS) (First Link, Wolverhampton, United Kingdom, UK), penicillin (100 U/ mL), streptomycin (100 μg/ml), and heparin (15 U/mL). For the first four days in culture, pBEC were selected using puromycin (4 μg/mL). At 70 % confuency, cells were passed with Trypsin/EDTA (2.5 % trypsin, 0.1 nM EDTA in PBS) and seeded on type IV collagen (500 μg/mL) and fibronectin (100 μg/mL) coated Transwell inserts (12 mm, 0.4 μm pore polycarbonate membrane, cat. no, 3401, Corning, Kennebunk ME 04043, USA) at a density of 1.1×10^5 cells/insert. pBECs were co-cultured with astrocytes in the basal chamber in serum-free media. To further induce the barrier development, both chambers were supplemented with the differentiation factors hydrocortisone (550 nM), 8-(4-chlorophenylthio)-adenosine-3′,5′-cyclic monophosphate (250 μM), and RO-201724 (17.5 μM) 1–2 days before experiments. The tightness of the model was validated by measurements of transendothelial electrical resistance (TEER) using an EndOhm-12 measurement device (World Precision Instruments), with values>1000 Ω cm^2 accepted for experiments. Before all experiments, Transwell inserts with cultured pBECs were transferred to a new 12-well plate without astrocytes, washed twice with PBS, incubated with media without differentiation factors, and allowed to rest in the presence of 5 % CO_2 for 2 h at 37 °C, before further treatment. To investigate the effects of the L. *lactis* CFSs on the BBB, 0.5 mg/mL of each CFS was added in the apical compartment and incubated at 37 °C, in the presence of 5 % CO2 up to 1–6-24 h with a circular rotation of 100 rpm and an orbit of 3 mm. The tightness of the barrier model was validated before and after the addition of the CFSs by measurements of TEER. Subsequently, for each time point, media from the top and the bottom were collected and stored at −20 °C for further analysis. Furthermore, the expression of adherens junction proteins was

validated by immunocytochemistry according to the procedures described below. To test the cytotoxicity of these CFSs, Trypan blue exclusion test was performed on astrocytes as described above.

4.9. Immunofluorescence staining

BECs were fixed in 4 % paraformaldehyde in cytoskeleton buffer (50 mM PIPES, 50 mM NaCl, 5 % glycerol, 0.1 % NP-40, 0.1 % Triton X-100 and 0.1 % Tween 20) at RT for 20 min, washed 3 times with PBS, and permeabilized with 0.1 % Triton X-100 for 10 min and blocked in 2 % BSA for 30 min. For immunostaining, 5 μg/mL of antibodies anti α-p120 catenin (610,133, BD Transduction Laboratory), mouse α-claudin 5 (35–2500 Thermo Fisher Scientific), and Rabbit α ZO-1 (61–7300 Invitrogen) were applied for 1 h at RT. Filters were then washed 3 times in PBS at RT before 30 min incubation in the dark with 1:200 anti-mouse antibodies Alexa Fluor 488 (A32731 Life technologies) and 1:200 anti-rabbit antibodies Alexa Fluor 568 (A10042 Invitrogen). For nuclear staining, cells were incubated with 0.125 μg/mL Hoechst stain solution (Sigma-Aldrich) for 10 min at RT. Finally, membranes were mounted on microscope glass slides #1.5, with ProLong Diamond Antifade Mounting medium (Invitrogen, Thermo Fisher Scientific).

4.10. Confocal microscopy and image processing

Confocal imaging was performed using an Olympus IX-83 fluorescent microscope with a confocal spinning disk unit (Yokogawa) and a 60 × 1.2 NA objective. Pictures are presented as maximum-intensity z-stack projections unless other specific details are noted in figure legends. Image processing and spot segmentation analysis were performed using Fiji software(Dobens & Dobens, 2013).

4.11. Statistical analysis

All data presented are based on three independent experiments, performed in triplicate ($n = 9$). Statistical analyses and graph preparation were performed using GraphPad Prism (version 8.0, GraphPad Software). Data are expressed as mean values ± standard deviation (SD). Prior to hypothesis testing, data distribution was assessed using the Shapiro–Wilk test to verify normality.

Depending on the experimental design, statistical significance was evaluated using unpaired *t*-tests with Welch's correction, or one-way and two-way ANOVA. Appropriate *post hoc* tests were applied according to the comparison strategy: Tukey's or Sidak's multiple comparisons test for pairwise group comparisons, and Dunnett's test when comparing treatment groups to a single control.

Approval for animal experiments

This research was approved Aarhus University Animal Facility veterinarian committee.

CRediT authorship contribution statement

I. De Chiara: Writing – original draft, Methodology, Investigation, Data curation, Conceptualization. **A. Feola:** Writing – original draft, Methodology, Investigation. **M. Della Gala:** Investigation. **R. Marasco:** Writing – review & editing, Data curation. **M.S. Nielsen:** Writing – review & editing, Methodology, Conceptualization. **A. Porcellini:** Writing – review & editing, Data curation. **M. Grieco:** Writing – review & editing. **M.T. Gentile:** Writing – review & editing, Writing – original draft, Data curation, Conceptualization. **L. Muscariello:** Writing – review & editing, Writing – original draft, Project administration, Data curation, Conceptualization.

Funding

This research was funded by the European Union and Italian MIUR, Project BIONUTRA—PON 2014–2020 (Development of Nutraceuticals from Natural Sources), Grant Number PON ARS01_01166.

Declaration of competing interest

The authors declare that they have no known competing financial interests or personal relationships that could have appeared to influence the work reported in this paper.

Acknowledgment

This research was funded by the European Union and Italian MIUR, Project BIONUTRA—PON 2014–2020 (Development of Nutraceuticals from Natural Sources), Grant Number PON ARS01_01166 and Project PRIN 2022, Project code: 2022M7PFZS. We thank Annemette Boe Marnow and Donato Sardella for technical assistance.

Appendix A. Supplementary data

Supplementary data to this article can be found online at https://doi.org/10.1016/j.foodres.2025.117840.

Data availability

Data will be made available on request.

References

Abbott, N. J., Patabendige, A. A., Dolman, D. E., Yusof, S. R., & Begley, D. J. (2010). Structure and function of the blood-brain barrier. *Neurobiology of Disease, 37*(1), 13–25. https://doi.org/10.1016/j.nbd.2009.07.030

Abd Ellatif, S. A., Bouqellah, N. A., Abu-Serie, M. M., Razik, E. S. A., Al-Surhanee, A. A., Askary, A. E., … Mahfouz, A. Y. (2022). Assessment of probiotic efficacy and anticancer activities of Lactiplantibacillus plantarum ESSG1 (MZ683194.1) and Lactiplantibacillus pentosus ESSG2 (MZ683195.1) isolated from dairy products. *Environmental Science and Pollution Research International, 29*(26), 39684–39701. https://doi.org/10.1007/s11356-022-18537-z

Alves, S. R., Calori, I. R., Bi, H., & Antonio Claudio, T. (2023). Characterization of glioblastoma spheroid models for drug screening and phototherapy assays. *OpenNano, 9*, Article 100116. https://doi.org/10.1016/j.onano.2022.100116

Banna, G. L., Torino, F., Marletta, F., Santagati, M., Salemi, R., Cannarozzo, E., … Libra, M. (2017). GG: An overview to explore the rationale of its use in Cancer. *Frontiers in Pharmacology, 8*, 603. https://doi.org/10.3389/fphar.2017.00603

Bhatia, P., Bernier, M., Sanghvi, M., Moaddel, R., Schwarting, R., Ramamoorthy, A., & Wainer, I. W. (2012). Breast cancer resistance protein (BCRP/ABCG2) localises to the nucleus in glioblastoma multiforme cells. *Xenobiotica, 42*(8), 748–755. https://doi.org/10.3109/00498254.2012.662726

Boccellino, M., Galasso, G., Ambrosio, P., Stiuso, P., Lama, S., Zazzo, D., … Di Domenico, M. (2021). H9c2 cardiomyocytes under hypoxic stress: Biological effects mediated by sentinel downstream targets. *Oxidative Medicine and Cellular Longevity, 2021*, Article 6874146. https://doi.org/10.1155/2021/6874146

Chuah, L. O., Foo, H. L., Loh, T. C., Mohammed Alitheen, N. B., Yeap, S. K., Abdul Mutalib, N. E., … Yusoff, K. (2019). Postbiotic metabolites produced by Lactobacillus plantarum strains exert selective cytotoxicity effects on cancer cells. *BMC Complementary and Alternative Medicine, 19*(1), 114. https://doi.org/10.1186/s12906-019-2528-2

Cito, L., Indovina, P., Forte, I. M., Pentimalli, F., Di Marzo, D., Somma, P., … Giordano, A. (2015). pRb2/p130 localizes to the cytoplasm in diffuse gastric cancer. *Journal of Cellular Physiology, 230*(4), 802–805. https://doi.org/10.1002/jcp.24805

De Chiara, I., Marasco, R., Della Gala, M., Fusco, A., Donnarumma, G., & Muscariello, L. (2024). Probiotic properties of. *Foods, 13*(6). https://doi.org/10.3390/foods13060957

Della Valle, M., D'Abrosca, G., Gentile, M. T., Russo, L., Isernia, C., Di Gaetano, S., … Fattorusso, R. (2022). Polystyrene nanoplastics affect the human ubiquitin structure and ubiquitination in cells: a high-resolution study. *Chem Sci, 13*(45), 13563–13573. https://doi.org/10.1039/d2sc04434j

Di Zazzo, E., Feola, A., Zuchegna, C., Romano, A., Donini, C. F., Bartollino, S., … Porcellini, A. (2014). The p85 regulatory subunit of PI3K mediates cAMP-PKA and insulin biological effects on MCF-7 cell growth and motility. *ScientificWorldJournal, 2014*, Article 565839. https://doi.org/10.1155/2014/565839

Dobens, A. C., & Dobens, L. L. (2013). FijiWings: An open source toolkit for semiautomated morphometric analysis of insect wings. *G3 (Bethesda), 3*(8), 1443–1449. https://doi.org/10.1534/g3.113.006676

Eladwy, R. A., Alsherbiny, M. A., Chang, D., Fares, M., Li, C. G., & Bhuyan, D. J. (2024). The postbiotic sodium butyrate synergizes the antiproliferative effects of dexamethasone against the AGS gastric adenocarcinoma cells. *Frontiers in Nutrition, 11*, Article 1372982. https://doi.org/10.3389/fnut.2024.1372982

Elango, A., Nesam, V. D., Sukumar, P., Lawrence, I., & Radhakrishnan, A. (2024). Postbiotic butyrate: Role and its effects for being a potential drug and biomarker to pancreatic cancer. *Archives of Microbiology, 206*(4), 156. https://doi.org/10.1007/s00203-024-03914-8

Erasimus, H., Gobin, M., Niclou, S., & Van Dyck, E. (2016). DNA repair mechanisms and their clinical impact in glioblastoma. *Mutation Research, Reviews in Mutation Research, 769*, 19–35. https://doi.org/10.1016/j.mrrev.2016.05.005

Fares, J., Fares, M. Y., Khachfe, H. H., Salhab, H. A., & Fares, Y. (2020). Molecular principles of metastasis: A hallmark of cancer revisited. *Signal Transduction and Targeted Therapy, 5*(1), 28. https://doi.org/10.1038/s41392-020-0134-x

Gentile, M. T., Pastorino, O., Bifulco, M., & Colucci-D'Amato, L. (2019). HUVEC tube-formation assay to evaluate the impact of natural products on angiogenesis. *J Vis Exp (148)*.. https://doi.org/10.3791/58591

Ghasemi, M., Turnbull, T., Sebastian, S., & Kempson, I. (2021). The MTT assay: Utility, limitations, pitfalls, and interpretation in bulk and single-cell analysis. *International Journal of Molecular Sciences, 22*(23). https://doi.org/10.3390/ijms222312827

Hoyles, L., Snelling, T., Umlai, U. K., Nicholson, J. K., Carding, S. R., Glen, R. C., & McArthur, S. (2018). Microbiome-host systems interactions: Protective effects of propionate upon the blood-brain barrier. *Microbiome, 6*(1), 55. https://doi.org/10.1186/s40168-018-0439-y

Kvakova, M., Kamlarova, A., Stofilova, J., Benetinova, V., & Bertkova, I. (2022). Probiotics and postbiotics in colorectal cancer: Prevention and complementary therapy. *World Journal of Gastroenterology, 28*(27), 3370–3382. https://doi.org/10.3748/wjg.v28.i27.3370

Lanskikh, D., Kuziakova, O., Baklanov, I., Penkova, A., Doroshenko, V., Buriak, I., … Kumeiko, V. (2024). Cell-based glioma models for anticancer drug screening: From conventional adherent cell cultures to tumor-specific three-dimensional constructs. *Cells, 13*(24). https://doi.org/10.3390/cells13242085

Leo, D. E., Lazzeri, E., Governini, L., Cuppone, A. M., Colombini, L., Teodori, L., … Pozzi, G. (2023). Vaginal colonization of women after oral administration of Lactobacillus crispatus strain NTCVAG04 from the human microbiota. *Minerva Obstet Gynecol, 75*(5), 432–439. https://doi.org/10.23736/S2724-606X.22.05087-4

Li, H., Lei, B., Xiang, W., Wang, H., Feng, W., Liu, Y., & Qi, S. (2017). Differences in protein expression between the U251 and U87 cell lines. *Turkish Neurosurgery, 27*(6), 894–903. https://doi.org/10.5137/1019-5149.JTN.17746-16.1

Liu, L., Wu, J., Zhang, J., Li, Z., Wang, C., Chen, M., … Luo, C. (2012). A compatibility assay of ursolic acid and foodborne microbial exopolysaccharides by antioxidant power and anti-proliferative properties in hepatocarcinoma cells. *Journal of Food, Agriculture and Environment, 10*, 111–114.

Marasco, R., Gazzillo, M., Campolattano, N., Sacco, M., & Muscariello, L. (2022). Isolation and identification of lactic acid Bacteria from natural whey cultures of Buffalo and cow Milk. *Foods, 11*(2). https://doi.org/10.3390/foods11020233

Morley, K. L., Ferguson, P. J., & Koropatnick, J. (2007). Tangeretin and nobiletin induce G1 cell cycle arrest but not apoptosis in human breast and colon cancer cells. *Cancer Letters, 251*(1), 168–178. https://doi.org/10.1016/j.canlet.2006.11.016

Nakatsuma, A., Fukami, T., Suzuki, T., Furuishi, T., Tomono, K., & Hidaka, S. (2010). Effects of kaempferol on the mechanisms of drug resistance in the human glioblastoma cell line T98G. *Die Pharmazie, 65*, 379–383. https://doi.org/10.1691/ph.2010.9807

Nataraj, B. H., Ali, S. A., Behare, P. V., & Yadav, H. (2020). Postbiotics-parabiotics: The new horizons in microbial biotherapy and functional foods. *Microbial Cell Factories, 19*(1), 168. https://doi.org/10.1186/s12934-020-01426-w

Nielsen, S. S. E., Siupka, P., Georgian, A., Preston, J. E., Tóth, A. E., Yusof, S. R., … Nielsen, M. S. (2017). Improved method for the establishment of an in vitro blood-brain barrier model based on porcine brain endothelial cells. *J Vis Exp(127)*.. https://doi.org/10.3791/56277

Pagano, C., Coppola, L., Navarra, G., Avilia, G., Savarese, B., Torelli, G., … Bifulco, M. (2024). N6-isopentenyladenosine inhibits aerobic glycolysis in glioblastoma cells by targeting PKM2 expression and activity. *FEBS Open Bio, 14*(5), 843–854. https://doi.org/10.1002/2211-5463.13766

Pandit, R., Chen, L., & Götz, J. (2020). The blood-brain barrier: Physiology and strategies for drug delivery. *Advanced Drug Delivery Reviews, 165-166*, 1–14. https://doi.org/10.1016/j.addr.2019.11.009

Pijuan, J., Barceló, C., Moreno, D. F., Maiques, O., Sisó, P., Marti, R. M., … Panosa, A. (2019). Cell migration, invasion, and adhesion assays: From cell imaging to data analysis. *Frontiers in Cell and Development Biology, 7*, 107. https://doi.org/10.3389/fcell.2019.00107

Scott, E., De Paepe, K., & Van de Wiele, T. (2022). Postbiotics and their health modulatory biomolecules. *Biomolecules, 12*(11). https://doi.org/10.3390/biom12111640

Sebastián Domingo, J. J. (2017). Review of the role of probiotics in gastrointestinal diseases in adults. *Gastroenterología y Hepatología, 40*(6), 417–429. https://doi.org/10.1016/j.gastrohep.2016.12.003

Sharma, P., Kaur, S., Kaur, R., & Kaur, M. (2018). Proteinaceous secretory metabolites of probiotic human commensal. *Frontiers in Microbiology, 9*, 948. https://doi.org/10.3389/fmicb.2018.00948

Singh, N., Miner, A., Hennis, L., & Mittal, S. (2021). Mechanisms of temozolomide resistance in glioblastoma - a comprehensive review. *Cancer Drug Resist, 4*(1), 17–43. https://doi.org/10.20517/cdr.2020.79

Sivakumar, H., Devarasetty, M., Kram, D. E., Strowd, R. E., & Skardal, A. (2020). Multi-cell type glioblastoma tumor spheroids for evaluating sub-population-specific drug response. *Frontiers in Bioengineering and Biotechnology, 8*, Article 538663. https://doi.org/10.3389/fbioe.2020.538663

Song, D., Wang, X., Ma, Y., Liu, N. N., & Wang, H. (2023). Beneficial insights into postbiotics against colorectal cancer. *Frontiers in Nutrition, 10*, Article 1111872. https://doi.org/10.3389/fnut.2023.1111872

Toth, A. E., Siupka, P., Augustine, P., Venø, S. T., Thomsen, L. B., Moos, T., … Nielsen, M. S. (2018). The Endo-lysosomal system of brain endothelial cells is influenced by astrocytes in vitro. *Molecular Neurobiology, 55*(11), 8522–8537. https://doi.org/10.1007/s12035-018-0988-x

Vera-Santander, V. E., Hernández-Figueroa, R. H., Jiménez-Munguía, M. T., Mani-López, E., & López-Malo, A. (2023). Health benefits of consuming foods with bacterial probiotics, Postbiotics, and their metabolites: A review. *Molecules, 28*(3). https://doi.org/10.3390/molecules28031230

Waithe, O. Y., Peng, X., Childs, E. W., & Tharakan, B. (2024). Measurement of Transendothelial electrical resistance in blood-brain barrier endothelial cells. *Methods in Molecular Biology, 2711*, 199–203. https://doi.org/10.1007/978-1-0716-3429-5_16

Was, H., Borkowska, A., Bagues, A., Tu, L., Liu, J. Y. H., Lu, Z., … Abalo, R. (2022). Mechanisms of chemotherapy-induced neurotoxicity. *Frontiers in Pharmacology, 13*, Article 750507. https://doi.org/10.3389/fphar.2022.750507

Wu, J., Zhang, Y., Ye, L., & Wang, C. (2021). The anti-cancer effects and mechanisms of lactic acid bacteria exopolysaccharides in vitro: A review. *Carbohydrate Polymers, 253*, Article 117308. https://doi.org/10.1016/j.carbpol.2020.117308

Wu, Y., Zhang, G., Wang, Y., Wei, X., Liu, H., & Zhang, L. (2023). A review on maternal and infant microbiota and their implications for the prevention and treatment of allergic diseases. *Nutrients, 15*(11). https://doi.org/10.3390/nu15112483

Zhou, F., Cao, W., Xu, R., Zhang, J., Yu, T., Xu, X., … Zhao, C. (2019). MicroRNA-206 attenuates glioma cell proliferation, migration, and invasion by blocking the WNT/β-catenin pathway via direct targeting of frizzled 7 mRNA. *American Journal of Translational Research, 11*(7), 4584–4601.

Zou, Y., Wang, Y., Xu, S., Liu, Y., Yin, J., Lovejoy, D. B., … Shi, B. (2022). Brain co-delivery of Temozolomide and cisplatin for combinatorial glioblastoma chemotherapy. *Advanced Materials, 34*(33), Article e2203958. https://doi.org/10.1002/adma.202203958